UC Irvine
UC Irvine Previously Published Works

Title

Eddy viscosity modeling in the prediction of turbulent, backmixed combustion performance

Permalink

Journal

ISSN

Authors

Peck, RE
Samuelsen, GS

Publication Date

1977

DOI

Copyright Information

Peer reviewed

EDDY VISCOSITY MODELING IN THE PREDICTION OF TURBULENT, BACKMIXED COMBUSTION PERFORMANCE

R. E. PECK° AND G. S. SAMUELSEN

UCI Combustion Laboratory, School of Engineering, University of California, Irvine, California

The turbulent flowfield in a backmixed combustor is modeled analytically by simultaneously solving the governing partial differential conservation equations. An algebraic and a two-equation eddy viscosity model are employed in the numerical simulation to account for the turbulence transport processes. Predicted distributions of isothermal flow properties are systematically compared to experimentally obtained data to appraise the eddy viscosity models. In addition, predicted distributions of reacting flow properties are presented to illustrate the applicability of current numerical methods to the prediction of continuous combustion flows.

The turbulent momentum and mass transport properties are evaluated in isothermal flow for a range of mixing conditions. Both eddy viscosity models qualitatively describe the system hydrodynamics, but the detailed flow structure is inadequately represented. The mass transport predictions from the algebraic viscosity model agree favorably with experiment. The inferior performance of the two-equation viscosity model is remedied by refining the boundary condition specification for the turbulence energy dissipation rate. It is shown that the turbulence energy dissipation rate adjacent to critical solid walls strongly influences the overall mixing characteristics of the two-equation model.

The isothermal flow results indicate that the algebraic eddy viscosity model provides cost-effective predictions of the general fluid flow patterns and mass transport trends in confined flows exhibiting strong recirculation. The two-equation eddy viscosity model provides better resolution of the small-scale turbulence processes but requires careful testing to ensure realistic predictions.

The hot flow calculations accentuate the inadequate transport characteristics identified in the isothermal flow analysis and verify that considerable testing of the numerical model is required before proceeding to the complicating conditions of combustion.

Introduction

The design and operation of continuous combustion devices such as gas turbines, boilers, and furnaces may be assisted by the development and application of suitable predictive models that account for pollutant production, combustion efficiency, and heat release behavior. The emergence of continuum flow models formulated from governing conservation equations represents a significant

° Present Address: Department of Mechanical Engineering, University of Kentucky, Lexington, KY 40506.

advance toward the numerical prediction of combustion-chamber performance. The application of continuum models to the design of combustion hardware is attractive because the point-by-point prediction of velocity, temperature, and composition is an integral part of the computational procedure. The quantitative prediction of turbulent, backmixed combustion has not yet been achieved because of uncertainties linked to the submodels of fundamental combustion processes. The present study addresses an essential element of continuum flow modeling—the use of eddy viscosity submodels to account for turbulence transport processes. The objective is to determine the utility and applicability of eddy viscosity submodels in the numerical simula-

tion of flows exhibiting strong recirculation or backmixing.

Approach

Selected eddy viscosity submodels are systematically evaluated in a combined analytical and experimental investigation. A backmixed laboratory combustor is employed to conduct tests for both isothermal (nonreacting) and hot (reacting) flow conditions. For the case of isothermal flow, the eddy viscosity submodels are first evaluated for the prediction of system hydrodynamics. A tracer gas is subsequently introduced to evaluate the eddy viscosity submodels for nonuniform, multicomponent flow where mass as well as momentum exchange is important. Experimental measurements and numerical predictions of velocity and tracer isopleths for a range of approach velocities and backmix characteristics provide the critical tests.

The results reported here emphasize the case of isothermal flow. A satisfactory assessment and understanding of the isothermal case is a prerequisite to engaging the hot flow case. Combustion imposes the additional requirement for submodels of chemistry and turbulence/chemistry interaction that may mask fundamental deficiencies in the eddy viscosity submodel. However, hot flow results are presented as an indication of the suitability of the two eddy viscosity submodels in the prediction of reacting flows.

The results provide useful information for the development of applied computational tools for analyzing the performance of continuous combustion systems. In particular, the results identify strengths and weaknesses in the use of two eddy viscosity submodels, and demonstrate the need to thoroughly test predictive methods for the case of isothermal flow before proceeding to the case of hot flow.

Combustion System

The experimental configuration is a 51 mm I.D. × 457 mm cylindrical Vycor combustion chamber containing an aerodynamic (opposed-jet) flameholder as shown in Fig. 1. The incoming flow of premixed methane and air is opposed by a high velocity jet ($\dot{m}_j/\dot{m}_m \ll 1$) issuing from a 1.3 mm I.D. (6.4 mm O.D.) water-cooled tube. The jet is coincident with the combustor axis and located 80 mm upstream from the combustor exit. The backmixed zone required for flame stabilization is generated along the jet boundary.
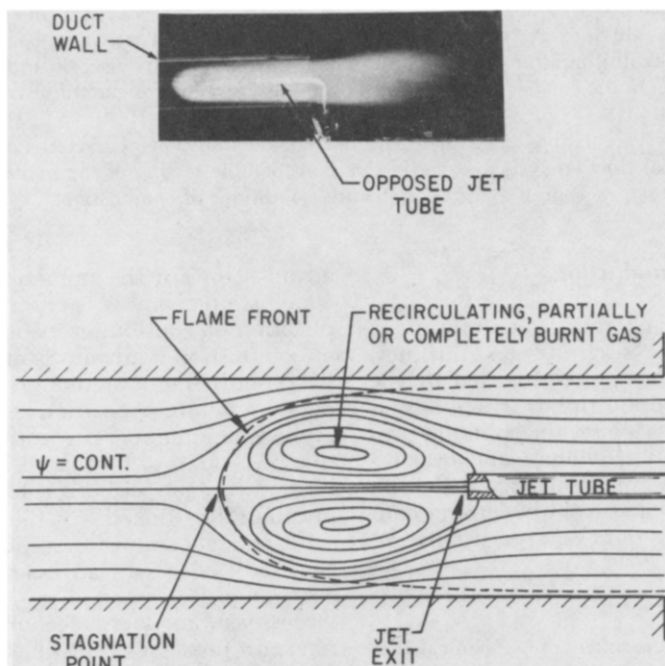

FIG. 1. Opposed-jet combustor flowfield schematic

The opposed-jet combustor (OJC) exhibits essential features found in practical continuous combustion systems (backmixing, high intensity combustion) but avoids the attendant complexities (nonpremixed, two phase combustion) appropriate for subsequent studies. The separation of the critical backmixing regime from influential boundary conditions is important to testing the eddy viscosity submodels. In addition, the OJC provides a versatile flowfield to challenge the predictive method. For example, the rate and intensity of backmixing in the recirculation zone may be altered experimentally and numerically over a broad range by varying the ratio of approach velocity to jet velocity.

Numerical Method

The theoretical analysis of the opposed-jet combustor is accomplished by solving numerically the time-averaged conservation equations for turbulent, backmixed flow with provision for chemical reaction. The backmixing requires that the governing mass, momentum, energy, and species conservation equations be elliptic. The computational procedure used to solve simultaneously the elliptic partial differential equations for the backmixed flowfield is based upon the TEACH method described by Gosman et al.[1] Equations containing the primitive $(p - \bar{V})$ variables are solved simultaneously to generate an isothermal flow solution. Equations for stagnation enthalpy $(\bar{h})$ and species mass fraction (Y_i) are then added to obtain a solution for hot flow conditions. The dependent variables (ϕ) are cast into a generalized equation of the form:

$$\frac{\partial}{\partial x}(\rho U\phi) + \frac{1}{r}\frac{\partial}{\partial r}r(\rho V\phi) = \frac{\partial}{\partial x}\left(\Gamma_{t,\phi}\frac{\partial\phi}{\partial x}\right)$$
$$+ \frac{1}{r}\frac{\partial}{\partial r}\left(r\Gamma_{t,\phi}\frac{\partial\phi}{\partial r}\right) + S_\phi \quad (1)$$

where $\Gamma_{t,\phi}$ and S_ϕ represent the turbulent exchange coefficient and source terms respectively. Boundary conditions are prescribed for all dependent variables following the recommendations of Ref. (1). After specification of inlet and solid boundary conditions, the finite difference calculations are carried out line-by-line over an 18×31 nonuniform grid covering the half-plane of the axisymmetric flowfield.

Turbulence Submodels

Turbulent transport properties are evaluated using time-mean or "effective" quantities.

This approach is standard practice in engineering calculations of turbulent flows and encompasses the introduction of turbulent exchange coefficients that imply Newtonian stress-strain relationships, Fourier heat conduction, and Fickian diffusion. A turbulent "eddy" viscosity, μ_t, is used to prescribe the turbulent momentum flux, i.e.

$$-\rho\,\overline{u'v'} = \mu_t\left(\frac{\partial U}{\partial r} + \frac{\partial V}{\partial x}\right) \quad (2)$$

The turbulent transport of scalar quantities is related to the eddy viscosity through the appropriate Prandtl or Schmidt numbers as follows:

$$\Gamma_{t,\phi} = \frac{\mu_t}{\sigma_{t,\phi}} \quad (3)$$

The present study explores specification of the eddy viscosity, μ_t, and turbulent mass transport, $\Gamma_{t,i}$, in confined flows exhibiting strong backmixing or recirculation. Comparative calculations are performed using two distinct turbulence submodels to define the eddy viscosity—an algebraic model and a more sophisticated two-equation submodel:

Algebraic[2]
$$\mu_t = KD^{2/3}\,L^{-1/3}\rho^{2/3}\,(mU^2)^{1/3} \quad (4)$$

K = empirical coefficient
D = diameter of combustor
L = length of combustor
ρ = local density
mU^2 = inlet kinetic energy

Two-Equation[3,4]
$$\mu_t = c_\mu\,\rho\,k^2/\epsilon \quad (5)$$

c_μ = empirical coefficient
ρ = local density
k = local turbulent kinetic energy
ϵ = local turbulent energy dissipation rate

The algebraic formulation is commonly used in predictive modeling. The variation in eddy viscosity depends only upon local density (spatially invariant for isothermal conditions) for a given geometry and inlet flow rate. The two-equation submodel introduces additional dependent variables that complicate the numerics and add computational cost. However, the two-equation submodel accounts for spatial variations in turbulent kinetic energy and

length scale, and has been tested satisfactorily in a number of fluid dynamic encounters.[5]

Results (Isothermal Flow)

To effectively test the submodels of eddy viscosity over a range of turbulent conditions, experimental data were obtained for approach velocities of 15.24 and 7.62 m/sec and jet velocities of 30.5, 61 and 130 m/sec. Velocity profiles were mapped throughout the flowfield using a 1 mm O.D. pitot tube. Tracer profiles were generated by introducing alternatively pure carbon monoxide (CO) in the jet and pure carbon dioxide (CO_2) in the mainstream. The mixing between the jet and mainstream was assessed by mapping CO and CO_2 profiles throughout the flowfield using a 3 mm O.D. stainless steel tube and Beckman 315B NDIR instruments for the gas sampling and analysis. The probe dimensions are small (probe O.D./OJC I.D. = .06) to minimize hydrodynamic interferences. The Reynolds number of the approach stream ranged from 2.5×10^4 (at 7.62 m/sec) to 5.0×10^4 (at 15.24 m/sec).

Momentum Transport

The eddy viscosity submodels were first tested for a homogeneous, isothermal flowfield to explore the effectiveness of the submodels in predicting momentum transport. Experimental and predicted profiles of the axial component of mean velocity are presented in Fig. 2 for an average inlet velocity of 15.24 m/sec. The selected profiles emphasize the flow regime dominated by recirculation. The velocity data are subject to experimental errors on the order of five percent in the bulk flow region, but in the recirculation zone the results are compromised by pitot tube errors of twenty-five percent or more. The calculated velocity profiles for both turbulence submodels assume an experimentally determined velocity profile as an inlet condition.

The trend of the velocity profiles agree qualitatively with the experimental results. The two-equation submodel retains the inlet turbulent velocity profile in the approach section while the velocity profiles predicted by the algebraic submodel flatten out due to the spatially uniform viscosity. The presence of the opposing-jet is communicated further upstream for the two-equation submodel than for the algebraic eddy viscosity, and the two-equation submodel demonstrates better correlation with the experimentally observed stagnation point.

The mean velocity profiles in the recirculation zone are also better represented by the two-equation turbulence submodel, although both submodels over-predict the jet expansion. In addition, the two-equation velocity profiles decrease too rapidly near the chamber wall. Downstream from the backmixed zone both submodels fail to adjust for the redistribution of the bulk flow in the turbulent wake of the recirculation zone and under-predict the velocity adjacent to the jet wall. Both submodels display good agreement in the bulk flow regime in the absence of recirculation or wall effects.

The recirculation zone strength was examined by reducing the approach velocity by a factor of two while retaining the same jet velocity. The experimental and predicted velocity profiles are presented in Fig. 3. The calculated results demonstrate a significant departure from experiment in the region of strong backmixing. The reverse flow region again penetrates further upstream in the two-equation submodel prediction.

The acceleration of the bulk flow around the recirculation zone is under-predicted in contrast to the over-predicted jet expansion for both submodels. This result is especially evident near the plane of the jet exit where the redistribution of the bulk flow with the jet discharge is restricted. This effect is conveyed downstream from the recirculation zone where the two-equation velocity profiles correlate well with experiment near the chamber wall but deviate near the jet wall.

Mass Transport

The two eddy viscosity submodels were secondly tested in conjunction with the turbulent mass exchange submodel (Eq. 3) for the conditions of an isothermal, nonhomogeneous flowfield. Spatial distributions of the predicted tracer concentrations are compared to experimental measurements in Figs. 4 and 5 for the baseline conditions outlined previously. The tracer gas concentration data were obtained at radial increments of 1.3 mm and axial stations every 13 mm. The concentration isopleths (experimental) were constructed from values measured at the discrete data points in the experimental flowfield and compared to concentration isopleths (predicted) constructed from values predicted at the discrete grid points in the computational field.

Figure 4 presents the algebraic and two-equation submodel predictions, and experimental tracer concentration distributions for a 15.2 m/sec average inlet velocity. (The jet
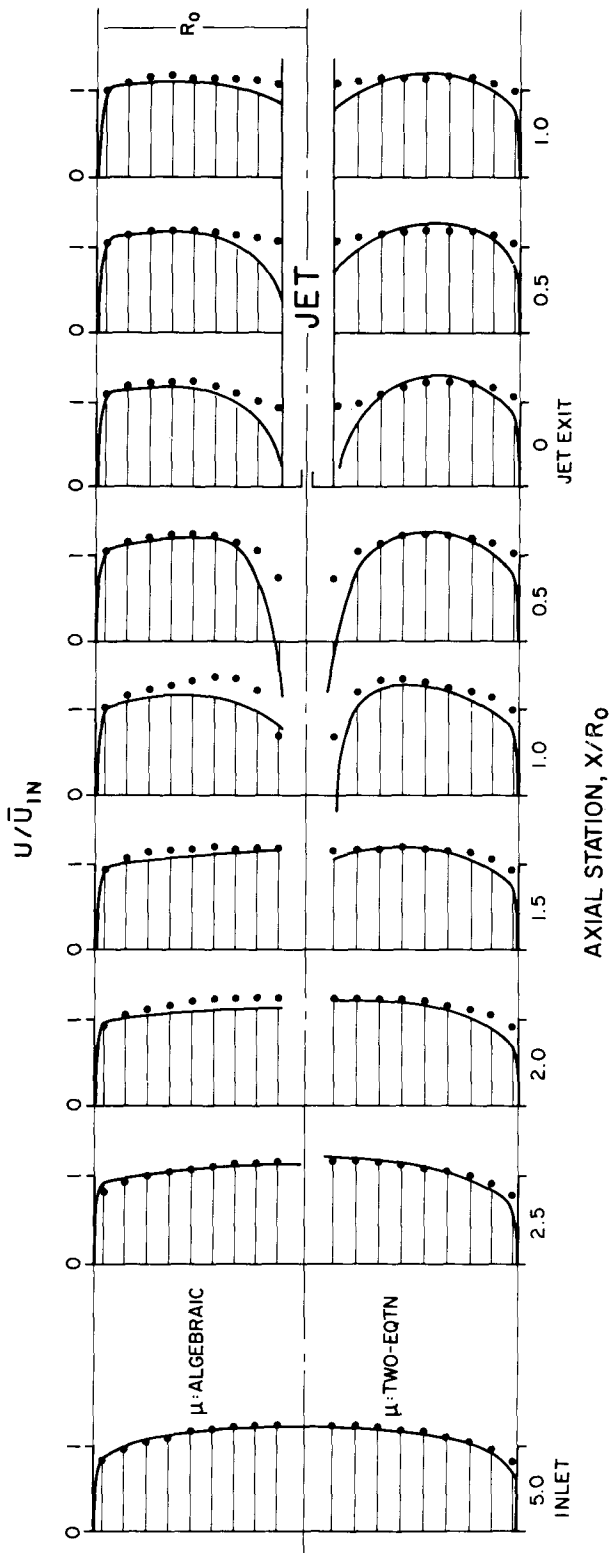
FIG. 2. Isothermal flow velocity profiles ($-$ predicted, $\cdot$ experimental). $\bar{U}_m = 15.24$ m/sec; $\bar{U}_j = 130$ m/sec; $\Phi_m = \Phi_j = 0$.
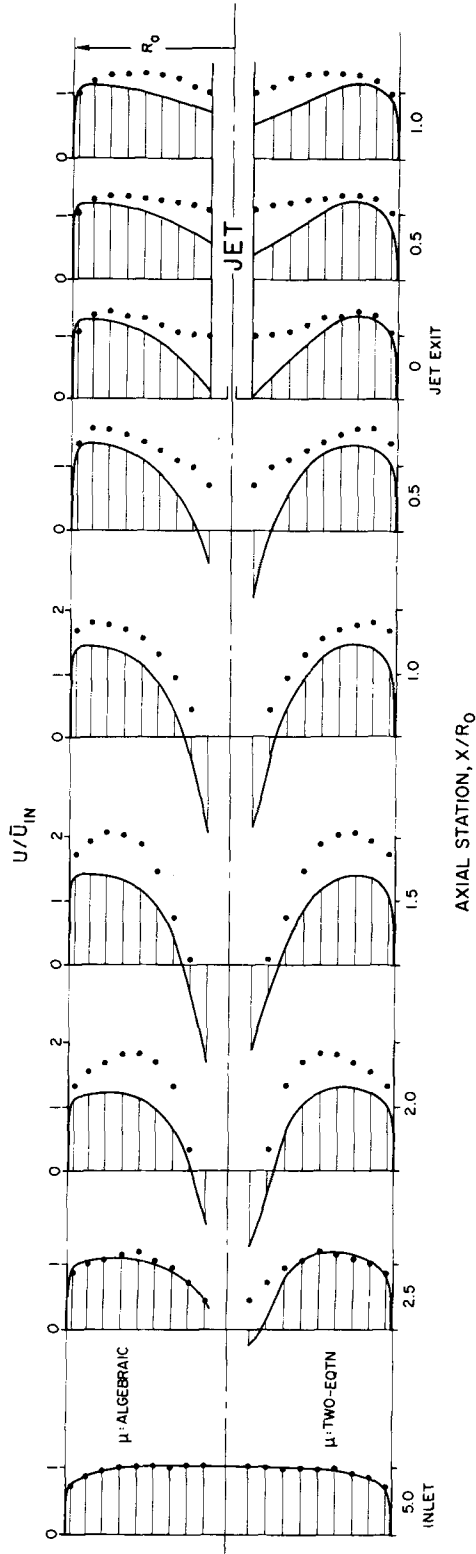
FIG. 3. Isothermal flow velocity profiles (- predicted, • experimental). $\bar{U}_m = 7.62$ m/sec; $\bar{U}_j = 130$ m/sec; $\Phi_m = \Phi_j = 0$.
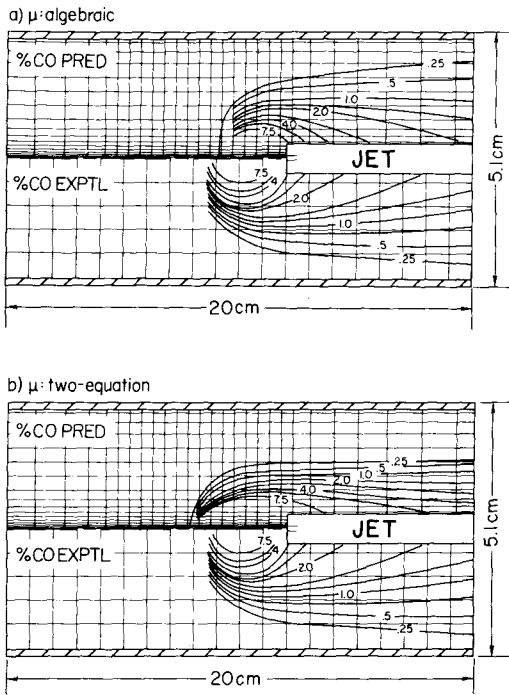
a) μ: algebraic

b) μ: two-equation

FIG. 4. Isothermal flow tracer concentration profiles. $\bar{U}_m$ = 15.24 m/sec; $\bar{U}_j$ = 130 m/sec; Φ_m = 0.; 100% CO Jet.

a) μ: algebraic

b) μ: two-equation

FIG. 5. Isothermal flow tracer concentration profiles. $\bar{U}_m$ = 7.62 m/sec; $\bar{U}_j$ = 130 m/sec; Φ_m = 0.; 100% CO Jet.

stream is 100 percent carbon monoxide.) Immediately evident is the contrasting axial and radial spread of the predicted tracer concentration profiles. Differences in axial transport of CO are consistent with the observations forwarded in the previous section on momentum transport. More notable are the diverse radial transport predictions. The spreading of the jet discharge into the mainstream for the algebraic eddy viscosity conforms to the experimental results. In contrast, the two-equation submodel limits the radial mixing of the jet stream (tracer) with the bulk flow. The segregation of the jet and the mainstream is verified by the high CO concentrations along the jet wall, in contrast to the absence of CO near the chamber wall. This result was further substantiated by introducing a carbon dioxide (CO_2) tracer in the approach stream. The numerical analysis of CO_2 concentrations for the two-equation submodel predict negligible mass transport of CO_2 from the mainstream into the recirculation zone. Downstream, the predicted mixing of CO_2 from the bulk stream into the flow associated with the jet stream is minor. Experimentally CO_2 was observed to be well mixed into the jet.
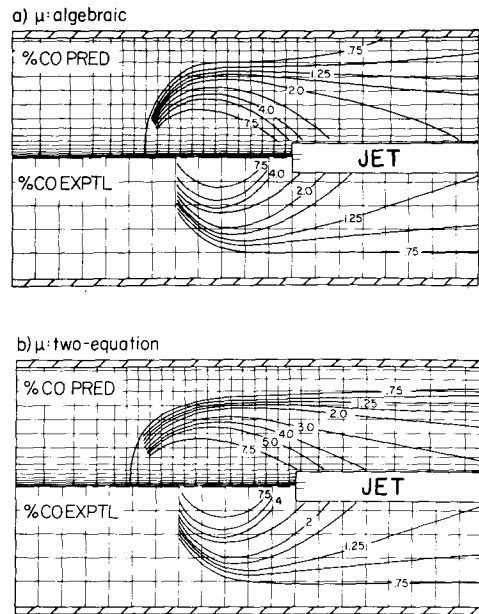
The results for the strong recirculation zone (Fig. 5) demonstrate similar trends. Although the velocity data presented earlier in Fig. 3 gave poorer agreement for conditions of strong recirculation, the mixing is improved because of the enhanced backmixing.

Results (Hot Flow)

A two-step global reaction mechanism for methane oxidation was adopted for the present study to illustrate the applicability of current numerical methods to the prediction of continuous combustion flows, and to briefly explore the suitability of the eddy viscosity submodels for the case of hot flow:

$$CH_4 + O_2 \rightarrow CO + H_2O \qquad (6)$$

$$CO + O_2 \rightarrow CO_2 \qquad (7)$$
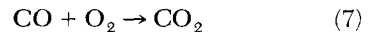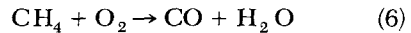
A detailed description of the numerical formulation of the reaction rate expressions and boundary conditions may be found elsewhere.[6] The dependent variables for the hydrocarbon system include the mass fractions Y_{CH_4} and Y_{CO_2}. Distributions of other major species— water (H_2O), oxygen (O_2) carbon monoxide (CO)—are related to Y_{CH_4} and Y_{CO_2} by elemental mass conservation. An initial solution

for the reacting flowfield was obtained using published reaction rates[7] which were later refined to more closely resemble the experimental data. This approach was justified on the basis that the reaction rate data were obtained from a well-stirred reactor study and may not apply to the current study, which deviates substantially from well-stirred conditions. Global reaction rates were judged acceptable for the present study because of the uncertainties encompassing the specification of the system aerodynamics.

Since the aim of the study is to predict the performance of backmixed combustion systems, the hot flow calculations were extended to include the prediction of the pollutant species, nitric oxide (NO). Nitric oxide kinetics were based on the familiar Zeldovich[8] mechanism:

$$O + N_2 \rightarrow NO + N \qquad (8)$$

$$N + O_2 \rightarrow NO + O \qquad (9)$$
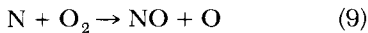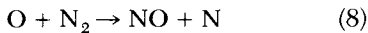
Noting that reaction (8) is the rate limiting step and adopting the simplifying assumption of O/O_2 equilibrium results in the reaction rate expression:

$$\frac{d[NO]}{dt} = 2 \, k_{8f} K_0 \, [N_2][O_2]^{1/2} \quad (10)$$

The temperature and O_2 distributions obtained from the solution of the hydrocarbon systems were used as a basis for the NO kinetic calculations.

The experimental tests conducted to complement the numerical predictions of hot flow properties utilized stoichiometric proportions of premixed methane and air in both the main and jet streams. The reactants were initially at ambient temperature and the combustion was completed at atmospheric pressure. The test matrix included the same approach velocities selected for the isothermal cases—7.62 and 15.24 m/sec—and a jet velocity of 130 m/sec.

Selected results of hot flow properties are presented in Figs. 6, 7, and 8 for the conditions indicated. Velocity, temperature, and NO data are presented as indicators of useful design information that may be derived from the numerical simulation of backmixed combustion processes. A photograph of the opposed-jet combustor is shown in Fig. 6 with predicted velocity vectors superimposed. The detailed maps of flowfield properties presented in Figs.
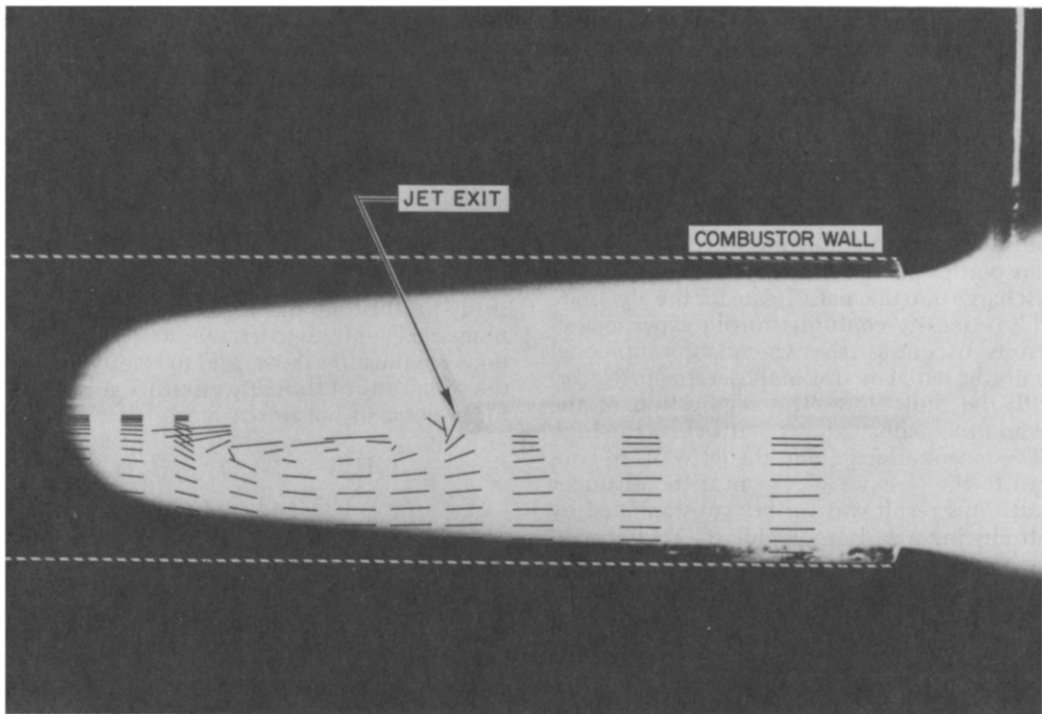

FIG. 6. Photograph of opposed-jet combustor burning premixed methane and air with predicted velocity vectors superimposed. $\bar{U}_m = 7.62$ m/sec; $\bar{U}_j = 130$ m/sec; $\Phi_m = \Phi_j = 1$.
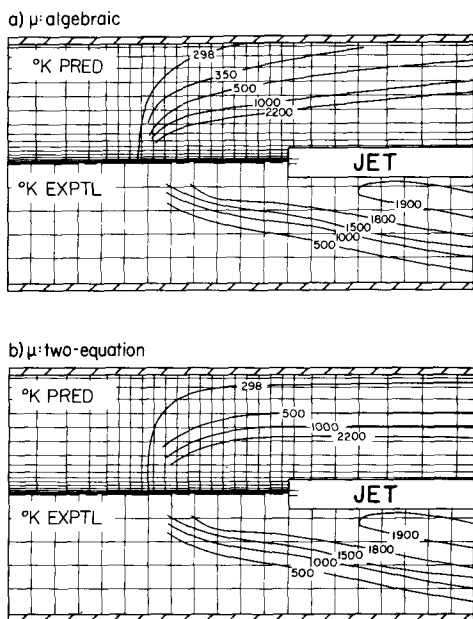
a) μ: algebraic

b) μ: two-equation

FIG. 7. Hot flow temperature distribution. $\bar{U}_m$ = 15.24 m/sec; $\bar{U}_j$ = 130 m/sec; $\Phi_m = \Phi_j = 1.0$.

a) μ: algebraic

b) μ: two-equation

FIG. 8. Hot flow nitric oxide concentration profiles. $\bar{U}_m$ = 15.24 m/sec; $\bar{U}_j$ = 130 m/sec; $\Phi_m = \Phi_j = 1.0$.

7 and 8 were obtained by conventional probing techniques. Temperature measurements were made using an uncoated Pt/Pt-13% Rh fine-wire thermocouple. The data are not corrected for radiation losses, but provide an adequate description of the OJC heat release distribution. A Scott Model 125 chemiluminescent analyzer was used for oxides of nitrogen measurements. Gas samples were extracted via a moveable 3.2 mm O.D. watercooled, 316 stainless steel probe having a tubular inlet, and conveyed through a heated teflon sample line to a packaged exhaust gas analysis system. The measurement of species susceptible to sample transformations (e.g. NO, NO_2) must be regarded as qualitative estimates of the actual local concentrations.

Discussion

Isothermal Flow

The results of the momentum and mass transport studies identify several important characteristics of the turbulence submodels. The turbulent viscosity from the two-equation submodel varies through the flowfield as is physically expected. The two-equation submodel also demonstrates the generation and dissipation of turbulence kinetic energy near the jet exit, the stagnation point and near the boundaries consistent with other numerical investigations.[9] In contrast, the turbulent viscosity from the algebraic submodel is spatially uniform throughout the flowfield for isothermal flow, and varies only with a change in the kinetic energy of the inlet streams. The impact of these differences between the two eddy viscosity submodels is evidenced by the velocity profiles, the predicted location of the stagnation point, the radial mass transport, and the dissipation of the kinetic energy of turbulence in the wake region.

Velocity Profiles. The predicted velocity profiles agree qualitatively with experimental results. The two-equation submodel more closely approximates the experimental trends although the predicted velocity contours for conditions of strong recirculation are quantitatively incorrect throughout the flowfield for both turbulence submodels. The departure from experiment is especially evident near walls, and suggests the need to refine the wall functions used to specify boundary conditions for turbulent kinetic energy or dissipation rate, and/or to decrease the grid spacing near the wall.

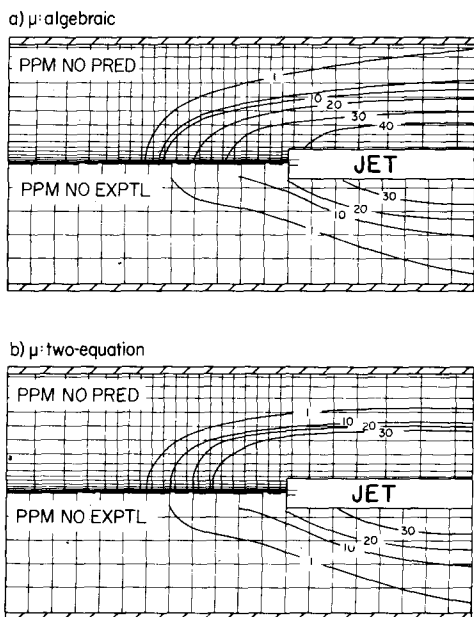*Stagnation Point.* The location of the

stagnation point as indicated by the velocity profiles and upstream extent of tracer measurements is better described by the two-equation submodel. The effective viscosity predicted by the algebraic submodel is spatially uniform through the flowfield for given inlet conditions. No account is made for changes in the kinetic energy of turbulence or energy dissipation rate in the region of encounter between the main and jet flows. The lower viscosity predicted in the recirculation zone by the two-equation submodel is more effective in describing the actual axial momentum and mass exchange.

Radial Mass Transport. Although the experimentally determined tracer isopleths are in closest agreement in the recirculation zone for the two-equation submodel, the downstream radial spread is more effectively described by the algebraic submodel. The uniformly high viscosity predicted by the algebraic turbulence submodel aids the overall mass transport throughout the flowfield, i.e. axial and radial diffusion from the jet is greater for the algebraic rather than for the two-equation submodel.

The radial mass transfer predicted by the two-equation turbulence submodel suggests that the principal mechanism of mass transport is by large-scale convection rather than by small scale gradient diffusion processes.[10] The tracer concentration varies gradually through the recirculation zone. The downstream mixing layer is bounded by steep concentration gradients that enclose the jet mixing region. The numerical predictions indicate that at high approach velocities the bulk flow detours around the recirculation zone, retaining upstream flow properties (low viscosity and small-scale mixing) and effectively precludes radially-directed mass transport. Conversely, the experimental trend reinforces the conjecture that turbulent exchange processes should be active throughout the annulus downstream from the recirculation zone.

Wake Region. The kinetic energy of turbulence predicted by the two-equation submodel is quickly dissipated in the wake region downstream of the recirculation zone. The resulting low viscosity impedes turbulent mixing throughout the wake region. In contrast, the uniformly high viscosity of the algebraic submodel is effective in predicting the radial spread of tracer observed experimentally.

Diagnosis

The results and subsequent discussion have exposed deficiencies in both of the eddy viscosity submodels that were tested and have identified directions for possible refinements. A supplementary investigation was initiated to determine the origin of the shortcomings of the two-equation eddy viscosity submodel in the present application and to improve the performance of the submodel in strongly recirculating flows.

A series of numerical experiments were conducted to examine the effect of boundary condition specifications on the turbulence transport characteristics of the two-equation eddy viscosity submodel for isothermal flow conditions. Turbulence properties at the jet and main stream inlets and adjacent to solid walls were systematically varied to improve numerical/experimental correlation and to determine the sensitivity of the solution to inlet and solid boundary conditions.

Modifications to the main inlet conditions, i.e. increased turbulence kinetic energy (k) and decreased turbulence energy dissipation (ϵ), improved the radial spread of tracer concentration but did not overcome the experimental discrepancies. The increased viscosity in the main stream also tended to move the predicted stagnation point downstream. Similar variations at the jet inlet had little impact on the radial mass transport but had a significant influence on the predicted stagnation point. Parametric changes reducing the viscosity in the vicinity of the jet exit tended to extend the stagnation point upstream.

The principal outcome of the parametric studies was the observation that in confined flows, where the recirculation zone may contact solid boundaries, the specification of near-wall turbulence energy dissipation rate may significantly influence the mixing characteristics of the two-equation turbulence submodel. These results are consistent with the findings of earlier studies[11] where a reduction of the energy dissipation rate adjacent to a downstream facing wall benefited numerical/experimental correlation. Similarly, the reduction of the energy dissipation rate on the upstream facing step of the jet tube was found to radically alter the predicted mass transport behavior of the two-equation submodel. The improved radial mass transport is evidenced by the tracer concentration profiles in Fig. 9. The stagnation point correlation may be restored by modifying the turbulence kinetic energy or the rate of turbulence energy dissipation at the jet inlet.

The analysis has shown that the turbulence energy dissipation rate in the flowfield is highly dependent on the shear stress along critical solid walls. The initially poor perform-
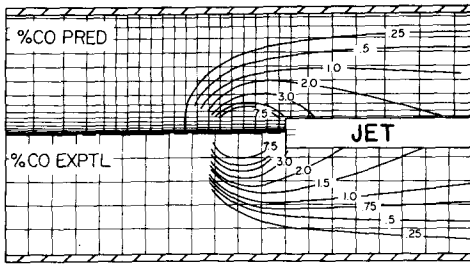
FIG. 9. Isothermal flow tracer concentration profiles for refined jet boundary conditions (μ: two-equation). $\bar{U}_m = 15.24$ m/sec; $\bar{U}_j = 130$ m/sec; $\Phi_m = 0.$; 100% CO Jet.

ance of the two-equation eddy viscosity submodel was remedied by refining the wall boundary conditions for the turbulence energy dissipation rate. The supplementary investigation has also demonstrated the need to test the two-equation turbulence submodel for isothermal flow conditions prior to simulating hot flows.

Hot Flow

The predicted hot flow results for the baseline eddy viscosity submodels qualitatively describe the bulk convective flowfield and the flameholding characteristics of the OJC, but the extent of chemical reaction is generally overestimated. The accelerated consumption of fuel and oxygen and the assumed adiabatic boundary conditions precipitate elevated flame temperatures and excess nitric oxide production. The spatial distributions of hot flow properties substantiate the inherent limitations of the eddy viscosity submodels that emerged in the isothermal flow analysis. The poor numerical simulation of the detailed flame structure is attributed to deficiencies in the coupled turbulence/chemistry submodels and the boundary condition specifications.

Conclusions

The relative merits of an algebraic and a two-equation eddy viscosity submodel for simulating turbulence transport properties in recirculating flows have been assessed by comparing continuum model predictions of the turbulent, backmixed flowfield in an opposed-jet combustor to experimental measurements.

Both eddy viscosity models qualitatively describe the bulk hydrodynamic flowfield, but

the detailed flow structure is inadequately represented. Mass transport estimates based on the algebraic viscosity model conform favorably to experiment. The two-equation turbulence submodel yields consistently poor correlation. The deficiency of the two-equation eddy viscosity model predictions is attributed to the boundary condition specification for the turbulence energy dissipation rate. It is shown that the turbulence energy dissipation rate adjacent to critical solid walls strongly influences the overall mixing characteristics of the two-equation submodel.

The results indicate that the algebraic eddy viscosity model provides cost-effective predictions of the general fluid flow patterns and mass transport trends in turbulent, confined flows exhibiting strong recirculation. The two-equation eddy viscosity submodel provides better resolution of small-scale turbulence processes but requires careful testing to ensure realistic predictions.

It is also shown that considerable testing of continuum flow models in isothermal flow is required before proceeding to the complicating conditions of combustion. The hot flow calculations accentuate the inadequate transport characteristics identified in the isothermal flow analysis. Attempts to refine the chemistry submodel or to quantify the interaction of fluid motions on chemical reaction rates are dependent on the correct turbulence submodel formulation.

Nomenclature

$\tilde{h}$	stagnation enthalpy
k	turbulence kinetic energy
$\dot{m}$	mass flowrate
p	pressure
r	radial coordinate
R_0	combustion chamber radius
U, V	mean velocity components
u', v'	fluctuating velocity components
$\bar{U}$	average velocity
x	axial coordinate
Y	mass fraction
Γ	exchange coefficient
ϵ	turbulence energy dissipation rate
μ	viscosity
ρ	density
σ	Prandtl or Schmidt number
ϕ	dependent variable
Φ	equivalence ratio

Subscripts

i	species
in	inlet

j	jet stream
m	main stream
t	turbulent

REFERENCES

1. GOSMAN, A. D. AND PUN, W. M.: Lecture notes for course entitled 'Calculation of Recirculating Flows.' Imperial College, Mech. Engrg. Dept., Report HTS/74/2, 1974.
2. GOSMAN, A. D., PUN, W. M., RUNCHAL, A. K., SPALDING, D. B. AND WOLFSHTEIN, M.: *Heat and Mass Transfer in Recirculating Flows*, p. 212, Academic Press, 1969.
3. LAUNDER, B. E. AND SPALDING, D. B.: *Mathematical Models of Turbulence*, p. 100, Academic Press, 1972.
4. JONES, W. P. AND LAUNDER, B. E.: Intern. J. Heat Mass Transfer, 15, 301, (1972).
5. LAUNDER, B. E. AND SPALDING, D. B.: The Numerical Computations of Turbulent Flows, Imperial College, Mech. Engrg. Dept., Report HTS/73/2, 1973.
6. SAMUELSEN, G. S. AND PECK, R. E.: Pollutant Formation in Reacting Flows with Recirculation, Paper 72-21, Western States Section/The Combustion Institute, Monterey, Calif., 1972.
7. WILLIAMS, G. C., HOTTEL, H. C. AND MORGAN, A. C.: *Twelfth Symposium (International) on Combustion*, p. 913, The Combustion Institute, 1969.
8. ZELDOVICH, YA. B., SADOVNIKOV, P. YA. AND FRANK-KAMENETSKII, D. A.: Oxidation of Nitrogen in Combustion, Academy of Sciences of USSR, Institute of Chemical Physics, Moscow-Leningrad, 1947.
9. KUBO, I. AND GOULDIN, F. C.: *Fluid Mechanics of Combustion*, p. 61, ASME, 1974.
10. SCHOFIELD, W. H. AND KEEBLE, T. S.: *Fluid Mechanics of Combustion*, p. 97, ASME, 1974.
11. MATTHEWS, L. AND WHITELAW, J. H.: The Prediction of Film Cooling in the Presence of Recirculating Flows with a 2-Equation Model of Turbulence, Imperial College, Mech. Engrg. Dept., Report HTS/71/31, 1971.

COMMENTS

D. B. Spalding, Imperial College, England. I would like to mention that the algebraic viscosity model is, I think, one invented by W. M. Pun and myself for an early demonstration of numerical combustion models. It was never expected to have wide use. That it has survived so long is due more to its attractive simplicity than to its validity or secure foundation.

Authors' Reply. We anticipated that the algebraic viscosity model would not survive the challenge to experiment. The two models were chosen with the expectation that the two-equation model would neatly resolve the deficiencies produced by the algebraic. That this did not occur in the present experiment should cause us all to pause and ponder the role simplicity should play in our methodology. Perhaps additional confrontation with experiment shall force the retirement of the algebraic model. Perhaps not.

●

Gary P. Schneyer, Science Applications, Inc., USA. I would like to commend the authors on their care and wisdom on proceeding first with isothermal cases and only then proceeding to combustion. I have a comment and a question. The comment is that for many "steady" combustion configurations, experiments show large-scale unsteady (often periodic) motions. For your configuration I would expect K-H waves to appear around the jet causing asymmetries if nothing else. These configurations can only be properly modelled by transient computer codes. Thus, your lack of agreement may be affected by non-turbulent, unsteady phenomena in your experiments so that your turbulent model may be better than you think (but maybe not).

The question is whether you measured different turbulent intensities in the burning vs. isothermal cases that were otherwise identical? If so, how did they differ?

Authors' Reply. At present there is no experimental evidence of large-scale, transient motions in the opposed-jet combustor flowfield. A laser velocimeter system is being incorporated into the OJC test facility to obtain isothermal and hot flow turbulence intensity measurements that have heretofore been unavailable. This information will broaden the data base for evaluating the turbulence submodels and will also facilitate exploring the interaction between fluid motions and chemical reaction rates in turbulent, backmixed combustion.

●

R. A. Duerr, NASA-Lewis Research Center, USA. Carbon monoxide has been previously used as a flow tracer in a high temperature oxidizing stream to study coaxial jet turbulence where the CO was converted to CO_2. In order to achieve reasonably accurate contours, relatively large amounts of CO should be used to ensure repeatability. Assuming that the same open duct apparatus was used for cold flow as well as hot flow, what was the flow rate of CO and what safety precautions were taken? The use of CO as a cold flow tracer can obviously be rather harmful to the experimenters over an extended test period. Other gases may be preferable from the standpoint of safety, such as carbon dioxide which would basically involve only a change in sample cells in the NDIR analyzer used in the test.

Authors' Reply. One hundred percent (100%) carbon monoxide (CO) is introduced as a tracer species through the jet for the isothermal conditions. Carbon dioxide (CO_2) is used as a tracer in the approach stream to allow simultaneous measurement throughout the flowfield of CO (from the jet) and CO_2 (from the main stream).

CO is purposefully selected for the jet tracer to minimize the total throughput of CO. For a maximum CO flowrate of 1g/sec, concentrations at the exit plane are less than those measured in the products of combustion for the reacting case. The venting system, designed for the reacting case, is adequate to protect experimenters from exposure to CO.

Tracer studies were not conducted for the case of hot flow in the present study.

●

John B. Fenn, Yale University, USA. The authors are to be complimented for their intrepid attempt to bridge the gap between measurements on and analysis of highly idealized combustion models and more realistic practical burners. I find particular satisfaction in their evidence that eddy transport plays a key and definable role in the behavior of ducted burners and provides a basis for characterizing their performance. During the previous gathering of this clan at MIT my then colleague Emory Wilkerson and I presented some results on the behavior of ducted ramjet burners.[1] They seemed clearly to show that measured values of eddy diffusivity in conjunction with a homogeneous reaction model for the combustion process were remarkably able to describe the dependence of combustion efficiency on pilot heat input and burner geometry. The present extension of those then primitive efforts is a progressive stride toward the goal of rational burner design.

REFERENCES

1. WILKERSON E., AND FENN, J. B.: *Fourth Symposium (International) on Combustion*, p. 749, Williams & Wilkins, 1953.